

Pongamia Pinnata (PP) shell powder filled sisal/kevlar hybrid composites: Physico-Mechanical and Morphological Characteristics

J Praveenkumara

UVCE: University Visveswarayya College of Engineering

Vidya Sagar H N

University Visvesvaraya College of Engineering

P Madhu

Malnad College of Engineering

Yashas Gowda

King Mongkut's Institute of Technology North Bangkok: King Mongkut's University of Technology North Bangkok

Sanjay Mavinkere Rangappa (✉ mcemrs@gmail.com)

King Mongkut's University of Technology North Bangkok <https://orcid.org/0000-0001-8745-9532>

Mohammad Rizwan Khan

King Saud University

Imran Khan

Aligarh Muslim University

Suchart Siengchin

King Mongkut's Institute of Technology North Bangkok: King Mongkut's University of Technology North Bangkok

Research Article

Keywords: Sisal, Kevlar, Pongamia pinnata (PP) shell powder, epoxy, SEM

Posted Date: March 11th, 2021

DOI: <https://doi.org/10.21203/rs.3.rs-273651/v1>

License: © ⓘ This work is licensed under a Creative Commons Attribution 4.0 International License.

[Read Full License](#)

1 **Pongamia Pinnata (PP) shell powder filled sisal/kevlar hybrid composites:**

2 **Physico-Mechanical and Morphological Characteristics**

3
4 **Praveenkumara J¹, Vidya Sagar H N¹, Madhu P², Yashas Gowda T G³, Sanjay M R^{3*},**
5 **Mohammad Rizwan Khan⁴, Imran Khan⁵, Suchart Siengchin³**

6
7 ¹Department of Mechanical Engineering, University Visvesvaraya College of Engineering,
8 Bangalore University, Bangalore, India.

9 ²Department of Mechanical Engineering, Malnad College of Engineering, Hassan,
10 Visvesvaraya Technological University, Belagavi, Karnataka, India.

11 ³Natural Composites Research Group Lab, Department of Materials and Production
12 Engineering, The Sirindhorn International Thai-German Graduate School of Engineering,
13 King Mongkut's University of Technology North Bangkok, Thailand.

14 ⁴Department of Chemistry, College of Science, King Saud University, Riyadh 11451, Saudi
15 Arabia.

16 ⁵Applied Sciences and Humanities Section, University Polytechnic, Faculty of Engineering
17 and Technology, Aligarh Muslim University, Aligarh – 202002, India.

18 *Corresponding Author: mcemrs@gmail.com

25 **ABSTRACT:** The composite industry is attracted by natural fiber reinforced polymer
26 materials for various valuable engineering applications due to its eco-friendly nature, less
27 cost, enhanced mechanical properties and thermal properties. This present work aimed at
28 incorporating sisal and kevlar woven fabrics with the epoxy matrix and to study the effect of
29 pongamia pinnata shell powder on this sisal/ kevlar hybrid composites. The six different
30 laminates were prepared using hand lay-up method with filler percentage varying 2 %, 4 %
31 and 6 %. The prepared laminates cut according to ASTM standards for performing different
32 mechanical tests. Results reveal that reduction of void percentage was observed at higher
33 filler contents, while the incorporation of kevlar fiber enhances the impact, tensile strength
34 and tensile modulus values. The flexural strength and inter laminar shear strength were higher
35 for 2 % filler composites, while the highest flexural modulus, hardness values were observed
36 for 6 % filler filled composites. The water absorption percentage was maximum for sisal
37 laminate (L-1) and minimum for kevlar laminate L-2. The fractured tensile and flexural
38 specimens were analyzed using scanning electron microscope (SEM).

39 **KEYWORDS:** Sisal, Kevlar, Pongamia pinnata (PP) shell powder, epoxy, SEM

40

41 **INTRODUCTION**

42 Natural fiber composites are the new class of engineering materials in composite industry
43 which are preferably used as lightweight, structural and semi-structural components in
44 automotive, constructional and building applications (Arpitha et al. 2017; Sanjay et al. 2018).

45 These natural fibers are the promising materials especially preferred in composite materials to
46 replace synthetic materials either partially or fully due to affordable class properties,
47 biodegradability, lower weight, good mechanical properties and renewable sources of
48 materials (Gowda et al. 2018; Madhu et al. 2019; Jothibasu et al. 2020). The plants which are
49 the sources of natural fibers are distinguished into two categories based on their applications.

50 The first category of plants such as hemp, jute etc., are utilized only for the extraction of
51 fibers, while the second category of plants such as pineapple, banana etc., are grown for fruit
52 farming and their byproducts and are used for extraction of fibers (Sanjay et al. 2019). Some
53 of the commonly used natural fibers include flax, kenaf, ramie, roselle, urena (bast fibers),
54 sisal, palm, bagasse, bamboo, coir, cotton, kapok (seed-hair and other fibers) (Elanchezian
55 et al. 2018; Thyavihalli Girijappa et al. 2019; Vinod et al. 2020). Sisal fiber belongs to the
56 *Agave sisalana* plant and their fibers are extracted from the leaves of this plant. The sisal
57 fiber cultivation was done by Maya, Indians and then by the Europeans and Brazil is the
58 highest sisal fiber producer country in the world. The major advantage of sisal fiber plant is it
59 can grow in any environment with any type of soil, highly potential, hard fiber and its yearly
60 percentage of production is high as compared to total textile production. Each sisal fiber
61 leaves consists of 87.25 % moisture, 4 % fiber, 0.75 % cuticle and 8 % dry matter (Rana et al.
62 2017; Damião Xavier et al. 2018; Naveen et al. 2019). Natural fibers are not having enough
63 properties to be used as prospective materials for high potential applications. To overcome
64 the negative aspects of natural reinforcements, the synthetic materials are preferred along
65 with natural fibers and synthetic fibers such as glass, carbon and kevlar fibers are the most
66 recognized materials from past few decades to be hybridized with various natural fibers.
67 Kevlar is one of the strongest, lightweight and heat resistant synthetic materials related to one
68 kind of aramid fibers. It has high tensile strength, tensile modulus, toughness and chemically
69 stable properties. It finds its applications in composite materials, aerospace engineering,
70 bulletproof materials and automotive parts (Fu et al. 2018; Amir et al. 2019). The method of
71 combining two or more types of fibers in a single matrix is termed as hybridization. This
72 efficient strategy increases the mechanical properties of the composites. The finer balancing
73 of mechanical properties are found in hybrid composites in comparison with non-hybrid
74 composites (Swolfs et al. 2014; Asim et al. 2017). Based on the requirement of properties and

75 type of applications different types of natural and synthetic fillers are used for enhancing the
76 properties of hybridized natural-synthetic composites. Natural fillers are bio-waste products
77 and some of the examples are eggshells, rice husk, coconut shell powder, peanut shell
78 powder, pongamia pinnata shell powder, fish bone and fish scale fillers. These natural fillers
79 increase the modulus, biodegradability and correspondingly decrease the composite cost and
80 matrix ductility. The polymer composites filled with natural fillers provides application in
81 several mechanical, tribological and industrial sectors (Mohan et al. 2012; Shakuntala et al.
82 2014; Jani et al. 2016).

83 S. Dinesh et al. conducted an experiment on wood dust filled jute fiber reinforced epoxy
84 composites. The proper distribution of wood dust particles and better adhesion with the
85 matrix resulted in improved mechanical properties. The water absorption percentage was less
86 in wood dust filled composite during 27 days of experiment (Dinesh et al. 2020). H. Singh et
87 al. studied the properties of fish bone powder (FBP) filled jute/carbon hybrid composites
88 under varying 0 - 5 wt. % of FBP powder. Addition of filler increased the contact surface
89 area and good adhesive nature resulting in enhanced tensile properties whereas flexural
90 strength showed declination value due to the ductility induced in the matrix which was
91 caused mainly because of filler material addition. The micro-hardness value diminished by
92 weak bonding occurring between fiber and matrix owing to less uniform distribution of filler
93 (Singh et al. 2020). V. Sharma et al. investigated the effect of fly ash particles (5%, 10% and
94 15%) on basalt fiber reinforced epoxy composites. The tensile, flexural and impact properties
95 are increased for 10 wt. % of filler whereas decreased for the filler wt. % from 10 to 15%. As
96 the filler weight increased, it was noticeable that the matrix was unable to transfer the load
97 effectively to the reinforcement (Sharma et al. 2020). Khalil et al. documented that the
98 optimum value of mechanical properties showed high density for 3 wt. % of coconut shell
99 filler filled kenaf/coconut fiber reinforced composites. This was due to incorporation of high-

100 density filler in low density matrix which resulted in the reduction of void content and
101 enhanced strength of the composites (HPS et al. 2017). Praveenkumara et al. incorporated
102 SiC particles in bamboo/carbon reinforced epoxy composites and reported that the prepared
103 composites showed higher tensile and hardness values as opposed to synthetic laminates and
104 indicated low water absorption in comparison with pure natural fiber laminates
105 (Praveenkumara et al. 2017). Prabu et al. documented that the red mud incorporated
106 sisal/banana fiber reinforced polyester composites revealed better flexural and impact
107 strength due to higher load withstanding capacity, while the tensile strength reduced because
108 of negligible stress interface between filler and matrix materials (Prabu et al. 2012).
109 Matykiewicz et al. investigated the mechanical and thermal properties of basalt powder filled
110 basalt fiber reinforced epoxy composites using hand lay-up method. The addition of 2.5 wt.
111 % basalt powder gives better stiffness and thermal resistive property to the prepared
112 composites. The tensile strength and modulus were higher whereas, the flexural strength
113 decreased for 2.5 wt. % filler laminate (Matykiewicz et al. 2017).

114 From the current literature survey, it is concluded that although many researchers
115 have worked on the hybridization of natural/synthetic hybrid composite and studied the effect
116 of natural fillers on these hybrid composites there are no works till date deliberated on
117 pongamia pinnata shell (PPS) powder filled sisal/kevlar hybrid composites. Thus, the present
118 study deals with the study of both hybridization and PPS filler material effect on sisal/ kevlar
119 hybrid composites. The void and weight percentage, mechanical properties (tensile, flexural,
120 impact, inter-laminar shear strength and hardness behavior) and water absorption studies have
121 been carried out to evaluate the prepared hybrid composites. Also, the micro structural
122 analysis of the fractured tensile and flexural specimens was scrutinized using scanning
123 electron microscopy (SEM).

124

125 **MATERIALS AND METHODS**

126 **MATERIALS USED**

127 In this present work, sisal and kevlar fibers are used as reinforcement materials and were
128 purchased from Go Green Products, Chennai, Tamilnadu and Composites Tomorrow,
129 Vadodara, Gujarat respectively. The parameters of sisal and kevlar fibers are tabulated in
130 **Table 1**. Epoxy resin CT/E-556 and CT/AH-951 polyamine hardener was also purchased
131 from Composites Tomorrow, Vadodara, Gujarat. For the matrix phase preparation epoxy and
132 hardener were mixed in 10:1 ratio. The bidirectional macroscopic view of sisal and kevlar
133 fabric are shown in **Figure 1 (a & b)**. Pongamia Pinnata shells were collected Pongame oil
134 tree and then seeds were removed from the shells which were later dried for 3-4 days in the
135 sun light. After the removal of moisture content, the shells were grinded to powder form.
136 **Figure 1 (c & d)** illustrates the pongamia pinnata shells (PPS) and PPS powder.

137

138 **Table 1.** Physical parameters of sisal and Kevlar fabrics

Parameters	Sisal	Kevlar
Woven style	Plain	Plain
Density (g/cc)	1.36	1.43
Weight (gsm)	160	220
Thickness (mm)	0.48	0.52
Warp yarns (yarns/m)	810	600
Weft yarns (yarns/m)	810	600

139



(a)



(b)



(c)



(d)

140 **Figure 1.** Materials used in the present study: (a) sisal fabric (b) kevlar fabric (c) Pongamia
141 pinnata shells (d) Pongamia pinnata shells powder

142

143 **2.2 PREPARATION OF COMPOSITE LAMINATES**

144 The composites of sisal, kevlar and PP filled laminates were fabricated using hand lay-up
145 method (Figure 2). The six types of different laminates of size $250 \times 250 \text{ mm}^2$ with total 4
146 layers of fabrics for each laminate has been maintained to achieve the thickness of 3 mm with
147 alternative sisal and kevlar fabric lay-up. The filler material was mixed with matrix phase by
148 the amount of 2, 4 and 6 wt. %. The sequence of fabric arranged along with weight fraction
149 percentage and volume fraction is as shown in Table 2. Granite slab is used as a flat mold
150 surface for the fabrication of laminates. Initially, silicone spray was sprayed on the bottom,

151 top and inner sides of the mold surfaces. Next, as per the laminate sequence, the fabrics were
 152 placed on the mold surface one by one by applying the epoxy uniformly using brushes and by
 153 the roller movements on the fabric to avoid the void formation. After completion of fabric
 154 lay-up, a wooden board of the mold size was placed along with the dead weights on the mold
 155 surface for the duration of 2 days. After 2 days in order to remove the moisture content, the
 156 laminates were placed inside the electric oven at 70⁰ C for 24 hours. Later the laminates were
 157 taken out from the oven and cut into ASTM standard dimensions for mechanical testing.
 158 In Table 2, w_f indicates the weight of the fabric {weight of sisal fabric (w_s) is 17 ± 1 g,
 159 weight of kevlar fabric (w_k) is 15 ± 1 g for the 250×250 mm² dimension fabric}, w_m
 160 indicates the weight of the matrix phase, w_{pps} is the weight of filler material. W_f is the weight
 161 fraction of fabric { W_s indicates weight fraction of sisal, W_k indicates weight fraction of
 162 kevlar}, W_m is the matrix phase weight fraction, w_{pp} is the weight fraction of filler material.

163

164 **Table 2.** Laminates sequence with weight and volume fraction

Laminates	Stacking sequence	Weight (g)				Weight fraction (%)				Volume fraction (%)
		w_f			w_m	W_f			W_m	
		w_s	w_k	w_{pp}		W_s	W_k	W_{pp}		
L-1	S+S+S+S	70 ± 3	—	—	170 ± 8	29.17	—	—	70	27.44
L-2	K+K+K+K	—	$60 \pm$	—	140	—	30	—	70	27.25

			3		±8				0	
L-3	S+K+S+K	34 ± 3	30 ± 3	—	160 ±8	15. 18	13 .4 0	—	7 1 .4 2	26.43
L-4	S+K+S+K + (2% PP)	34 ± 3	30 ± 3	2	160 ±8	15. 04	13 .2 7	0 .9	7 0 .7 9	27.21
L-5	S+K+S+K + (4% PP)	34 ± 3	30 ± 3	4	160 ±8	14. 91	13 .1 6	1 .8	7 0 .1 3	27.98
L-6	S+K+S+K + (6% PP)	34 ± 3	30 ± 3	6	160 ±8	14. 78	13 .0 4	2 .7	6 9 .4 8	28.7
<ul style="list-style-type: none"> S -Sisal fabric, K - kevlar fabric, PP - pongamia pinnata shell powder 										

165

166

167

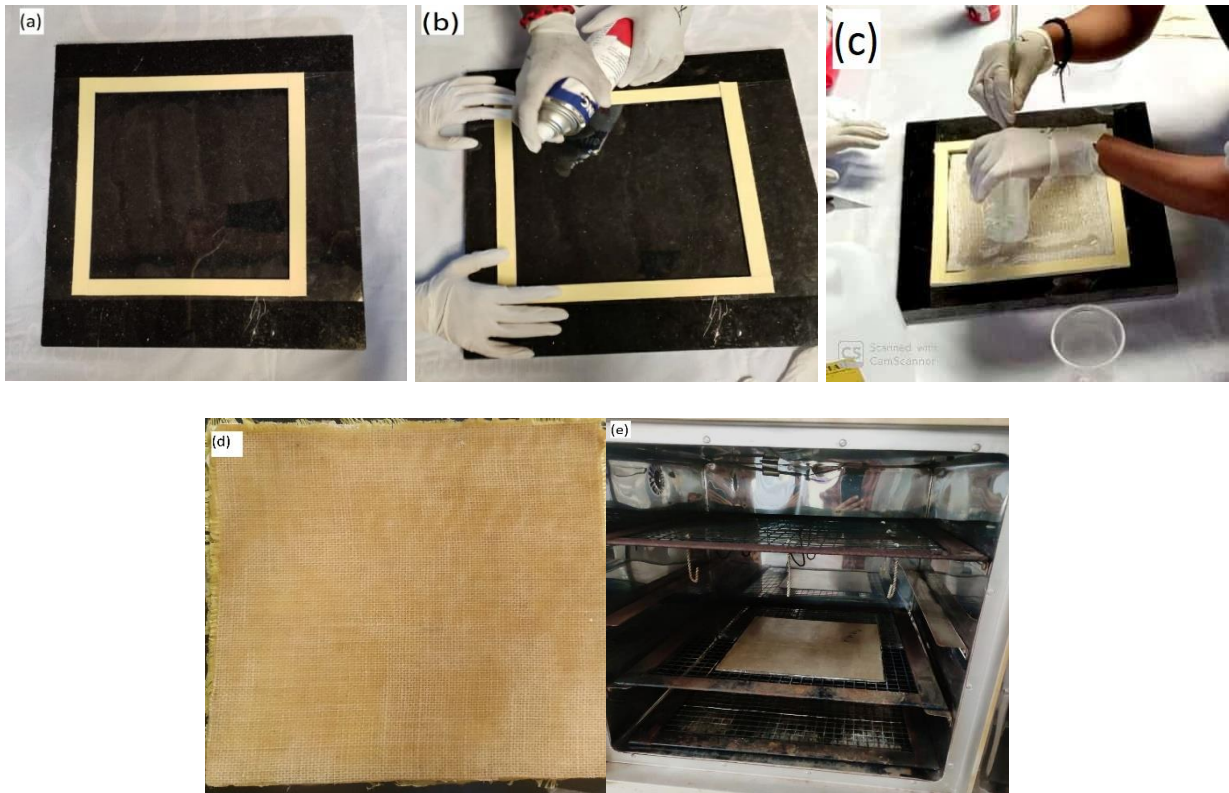
168 The weight fraction (%) of fiber and matrix is calculated by the equation (1)

169
$$W_f = w_f / (w_f + w_m) \text{ and } W_m = w_m / (w_f + w_m) \dots \dots \dots (1)$$

170 The total fiber volume fraction (%) is calculated by the equation (2)

171
$$V_f = \frac{\left(\frac{w_s}{\rho_s}\right) + \left(\frac{w_k}{\rho_k}\right) + \left(\frac{w_{pp}}{\rho_{pp}}\right)}{\left(\frac{w_s}{\rho_s}\right) + \left(\frac{w_k}{\rho_k}\right) + \left(\frac{w_{pp}}{\rho_{pp}}\right) + \left(\frac{w_m}{\rho_m}\right)} \dots \dots \dots (2)$$

172



173 **Figure 2.** (a) Mold prepared using sealing tape (b) Silicone spray (c) Resin lay up (d)

174 Fabricated laminate (e) Laminate curing in oven.

175

176 **EXPERIMENTAL STUDIES**

177 **DENSITY AND VOID FRACTION STUDIES**

178 The laminates were prepared according to ASTM D2734-94 method to find out the density

179 and void percentage of the prepared hybrid composites. The experimental density was

180 calculated using Archimedes principle by calculating the weight of the specimen in air and

181 liquid. The equation (3) was used for the calculation of experimental density (Ojha et al.
 182 2014).

183
$$\rho_{ex} = \frac{w_a}{w_a - w_l} \times \rho_l \dots \dots \dots (3)$$

184 Where ρ_{ex} represents experimental density, w_a represents weight of the specimen in
 185 air, w_l represents weight in liquid and ρ_l indicates density of the liquid.

186 The theoretical density was calculated for each laminate and six trials were conducted for the
 187 individual laminates and middle value was recorded. The theoretical density was calculated
 188 based on weight fraction using the equation (4) (Rajulu et al. 2004).

189
$$\rho_{th} = \frac{100}{\frac{W_m}{\rho_m} + \frac{W_f}{\rho_f}} \dots \dots \dots (4)$$

190 Where W_m indicates the weight fraction % of matrix phase, ρ_m represents the density of the
 191 matrix phase, W_f indicates weight fraction % of fiber and ρ_f indicates density of the fabric.

192 During the fabrication of composites, voids were induced due to the improper fabrication
 193 technique. The composite with below 1% voids is considered to be a good composite, while
 194 the laminates greater than 5% are considered to be poor ones. As the void percentage
 195 increases the properties of the composite show diminished values with lessening water-
 196 resistant property. The density and void fraction percentage is tabulated in **Table 3**. The void
 197 percentage was calculated using theoretical and experimental density using equation (5)
 198 (Arpitha et al. 2017) [29].

199
$$V_v = \frac{\rho_{th} - \rho_{ex}}{\rho_{th}} \dots \dots \dots (5)$$

200 Where v_v indicates void percentage, ρ_{th} indicates theoretical density and ρ_{ex} indicates
 201 experimental density.

202
 203

204 **Table 3.** Density and void fraction of laminates

Laminates	Theoretical density ρ_{th} (g/cc)	Experimental density ρ_{ex} (g/cc)	Void (%)
L-1	1.299	1.289	0.76
L-2	1.306	1.302	0.45
L-3	1.223	1.215	0.65
L-4	1.192	1.185	0.58
L-5	1.168	1.162	0.51
L-6	1.113	1.108	0.44

205

206

207 **TENSILE STRENGTH STUDIES**

208 The tensile strength and tensile modulus were calculated according to the ASTM D638-03
 209 (115×19×3 mm³) standard dimensions. The test was conducted using computerized universal
 210 testing machine (UTM) with a load cell capacity of 1000 Kg. The tests were conducted for
 211 six trials for each laminate under a fixed strain rate of 3 mm/min. **S1 (a)** and **(b)** envies the
 212 specimen before and after the test. Initially, the specimen was fixed in between the grippers
 213 provided and the deflections were noted down for each corresponding load. The load was
 214 applied till the specimen broke and the break load was noted for the calculation of ultimate
 215 strength of the composite.

216

217 **FLEXURAL STRENGTH STUDIES**

218 The flexural strength and flexural modulus were calculated as per ASTM D790-07 standard
 219 with a dimension of 90×10×3 mm³ using a same UTM machine. The three-point bending
 220 method was used with a constant strain rate of 1.15 mm/min. The flexural specimen before

221 and after test is shown in **S2 (a)** and **(b)**. For this test also six identical specimens were taken
222 from each laminate. The load was applied at the center of the gauge length and the ends were
223 supported by gripped jaws. Corresponding load v/s displacement and stress v/s strain graphs
224 were obtained.

225

226 **IMPACT STRENGTH STUDIES**

227 The impact strength of the laminates was carried out by computerized impact tester according
228 to ASTM D256 standard with a dimension $63 \times 12.7 \times 3 \text{ mm}^3$. The impact test specimen was
229 loaded in grippers of the impact tester and the amount of energy absorbed for the fracture of
230 specimen was recorded in joules. **S3 (a)** and **(b)** shows impact test specimens before and after
231 test.

232

233 **INTER-LAMINAR SHEAR STRENGTH (ILSS) STUDIES**

234 The ILSS test also called as short beam shear test (SBS) is one of the quality measures for
235 brittle matrix-based composites. This test was conducted as per ASTM D2344 standard with
236 specimen dimensions of $60 \times 10 \times 3 \text{ mm}^3$. The specimen was placed between the two
237 supports and the load is applied to the center of span length using three-point bending
238 method. During the loading of specimen, the shear stress exerts on the laminates and load-
239 displacement, stress-strain graphs were obtained at a loading rate of 1.15 mm/min. The ILSS
240 specimens before and after test are illustrated in **S4 (a)** and **(b)**. The ILSS strength was
241 calculated using peak load of the specimen.

242

243 **HARDNESS STUDIES**

244 The hardness of the specimen was obtained using a digital Shore-D hardness durometer. The
245 range of durometer is 0-100 HD with a step of 0.5 HD. It is specially used for testing the

246 hardness of polymer, plastics and rubbers. During testing, the durometer was pressed on the
247 surface, then the indenter pin penetrates the specimen and resistance to indentation was
248 displayed in digital form (Qi et al. 2003). If the HD value is above 60, it is considered as
249 good resilience material and below 60 is considered as poor resilience material.

250

251 **WATER ABSORPTION STUDIES**

252 The water absorption test was conducted by immersing the specimens under normal and
253 distilled water condition in the duration of 28 days. The test specimens were prepared as per
254 ASTM D570 standard with dimensions $30 \times 28 \times 3 \text{ mm}^3$. The specimens are shown in **S5**.
255 The specimen weights are measured in the interval of 7 days by removing the water
256 molecules on the specimen surface and weighed using precise digital balance. The water
257 absorption percentage was calculated using the equation (6) (Sanjay et al. 2016).

258
$$\text{Water absorption (\%)} = \frac{W_b - W_a}{W_a} \times 100 \dots\dots\dots(6)$$

259 where W_b is the weight of the specimen after 7 days of immersion and W_a is the weight of the
260 specimen before immersion.

261

262 **SCANNING ELECTRON MICROSCOPY (SEM) STUDIES**

263 The fractured surfaces of tensile and flexural specimens were studied by using Hitachi SU
264 3500 model SEM equipment. The ends of the fractured specimens were cut into less than 10
265 $\times 10 \times 3 \text{ mm}^3$ dimensions and their surfaces were uniformly coated with carbon and gold.
266 The morphology tests were carried out for the identification of voids, fiber pull-out in the
267 composite, voids, fiber-matrix interface, uniform mixing of filler contents in the matrix and to
268 understand the adhesive property behaviour between the reinforcement and matrix phase.

269

270

271 **RESULTS AND DISCUSSIONS**

272 **DENSITY AND VOID FRACTION**

273 The volume fraction (%) of voids in the composite laminate was obtained by the difference of
274 experimental and theoretical densities. A slight difference of theoretical and experimental
275 densities was observed in laminates. The laminate L-6 shows a lesser amount of voids
276 (0.44%) as compared to other laminates due to higher compatibility between reinforcement,
277 matrix and filler material. The laminate L-2 has 0.45% of voids which was slightly higher
278 than laminate L-2. The laminate L-1 contains 0.76% of voids fraction and was comprised of
279 only natural reinforcement. The six different composite laminates void fraction ranged
280 between 0 to 1%. This indicates that all composites were properly fabricated with acceptable
281 void percentage. By considering above test observations, it is concluded that the affiliation of
282 synthetic reinforcement and higher concentration of filler material reduces the void
283 percentage and leads to augmentation in properties.

284

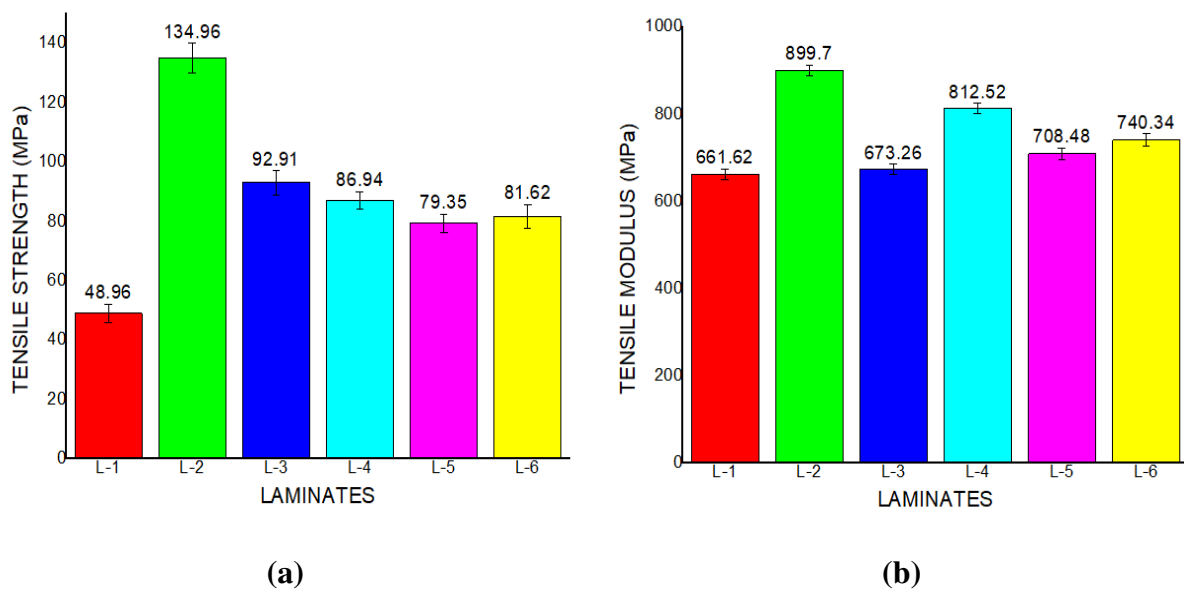
285 **TENSILE STRENGTH ANALYSIS**

286 The tensile properties of laminates L-1, L-2, L-3, L-4, L-5 and L-6 were studied using UTM
287 machine according to ASTM standard. The stress v/s strain curves for different laminates are
288 shown in **S6**. The laminate L-2 has higher yield stress as compared to other laminates and the
289 laminate L-1 has lower stress yield capacity. Laminate L-3 reaches second highest stress
290 value next to the L-2. Among PP filled composites, L-4 having 2% filler yields higher stress
291 value while its stress value decreased for L-5 and L-6. The tensile strength and tensile
292 modulus of different laminates were obtained by stress-strain raw data. Similarly load v/s
293 displacement graph was obtained and the same as been shown in **S7**. The composite having
294 only kevlar reinforcement (L-2) withstands higher tensile strength of 134.96 MPa and
295 modulus of 899.7 MPa. L-2 laminate which contains only natural sisal reinforcement

396 achieves tensile strength of 48.96 MPa and modulus of 661.62 MPa. The hybridized
397 composite of 2 layers sisal and 2 layers of kevlar fabric (L-3) obtained the strength of 92.91
398 MPa and 673.26 MPa of modulus value. By these observations, the composite with synthetic
399 fabric has achieved improvement in tensile strength value.

300 The tensile strength and tensile modulus values of different laminates are represented in
301 **Figure 3 (a) and (b)**. The hybridized laminate with 2% pp filled composite showed slightly
302 lesser tensile strength of 86.94 MPa and higher tensile modulus of 812.52 MPa as compared
303 to L-3. Further 4% pp filled composite displayed decreased strength of 79.35 MPa and
304 708.48 MPa of modulus values. The laminate L-6 has 81.62 MPa of tensile strength and
305 740.34 MPa of tensile modulus. By the observations, it is concluded that the laminate L-2 has
306 highest tensile and modulus values whereas hybridized composite (2 layers of sisal + 2 layers
307 of kevlar) with 2% filler shows an optimum tensile strength and modulus value. Hence
308 incorporation of synthetic kevlar fabric enhanced the tensile strength and the tensile modulus
309 with addition of 2% weight concentration of filler material.

310



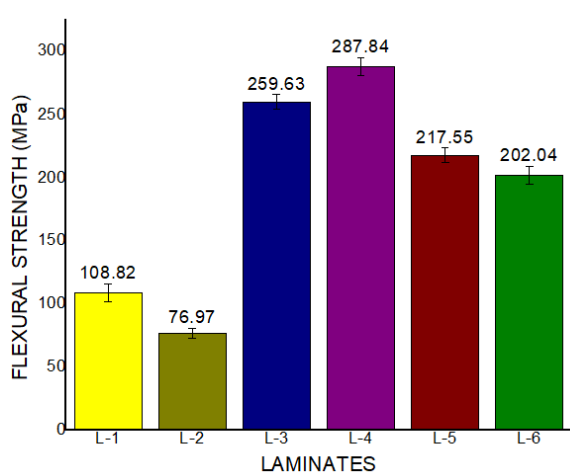
311 **Figure 3.** Tensile test results of the laminates: (a) Tensile strength (b) Tensile modulus

312

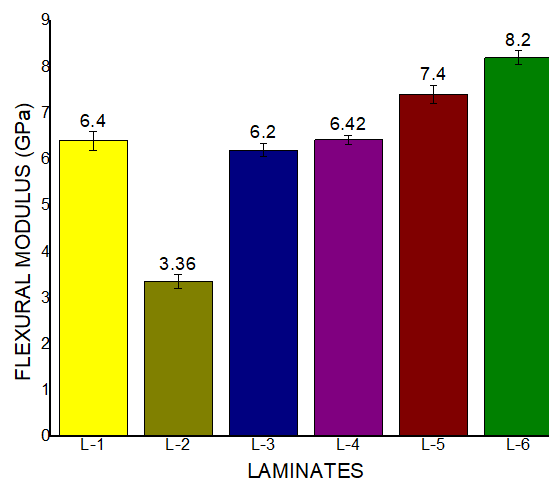
313 **FLEXURAL STRENGTH ANALYSIS**

314 **S8** and **S9** represents the stress-strain and load-displacement graphs respectively for flexural
315 specimens using three-point bending method. The laminate L-4 withstands a highest flexural
316 load of 348 N and least amount of flexural load was obtained for L-2 laminate. The peak
317 flexural loads for laminates L-5 and L-6 falls to 263 N and 244 N respectively because of
318 increase in filler concentration by the amount of 4% and 6%.The laminate L-1 has a
319 capability to withstand slightly higher load of 131 N as opposed to laminate L-2. During the
320 observations of load-displacement curve, the laminate L-2 material failure occurred at less
321 flexural load and then the displacement goes on increasing with decreasing load with long
322 time duration as compared to other laminates.

323 The flexural strength and flexural modulus for different laminates are characterized in **Figure**
324 **4** (a) and (b). The flexural strength indicated better adhesive properties between fiber-matrix
325 with the filler material. Among all the laminates, the hybridized laminate with 2% pp (L-4)
326 filler material had highest flexural strength of 287.84 MPa and moderate flexural modulus of
327 6.42 GPa. The least amount of flexural strength (76.97 MPa) and modulus (3.36 GPa) were
328 observed in L-2 laminate which was made of 4 layers of kevlar fabrics. The pure sisal fiber
329 reinforced laminate (L-1) envied a flexural strength of 108.82 MPa and modulus of 6.4 GPa
330 while, the hybridized 2 layered sisal and 2 layered kevlar laminate (L-3) withstands a flexural
331 strength of 259.63 MPa and modulus of 6.2 GPa. Further increased filler concentration by 4%
332 and 6% reduced the flexural strength by 217.55 MPa and 202.04 MPa respectively, at the
333 same time the modulus value was elevated to 7.4 GPa, 8.2 GPa for L-5 and L-6 laminates
334 respectively. Hence by these observations the flexural modulus was increased with increase
335 in filler concentration and the laminate L-4 with 2% filler gives optimum flexural properties.



(a)



(b)

336

337 **Figure 4.** Flexural test results of the laminates: (a) Flexural strength (b) Flexural modulus

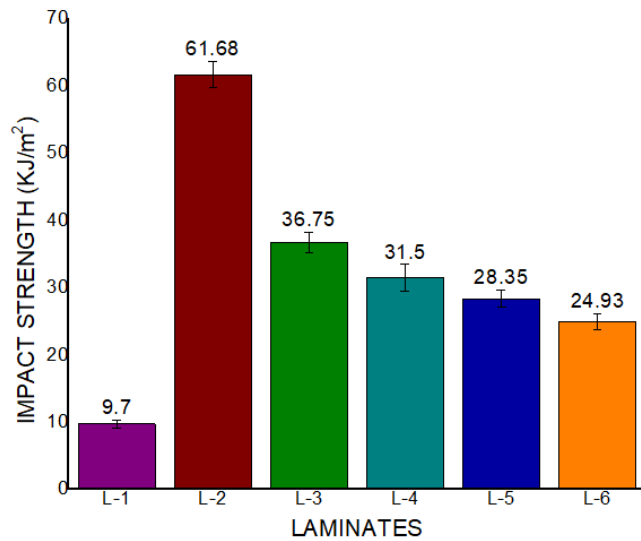
338

339 **IMPACT STRENGTH ANALYSIS**

340 The impact studies were conducted to determine the bonding strength of the fiber and matrix
 341 with the filler material. The impact strength (kJ/m^2) of the different laminates is presented in

342 **Figure 5.** The impact properties depend on the various parameters like stacking sequence,
 343 fiber matrix bonding, nature of the fiber material and geometry of the composites. The impact
 344 strength was calculated using the equation (vii). The laminate L-2 has higher impact strength
 345 of 61.68 kJ/m^2 as compared to other laminates which was due to higher stiffness of the kevlar
 346 fabric. The lower impact strength was found in laminate L-1 which has only sisal fabric
 347 reinforcement. The hemicellulose contents and less stiffness value resulted in deprived
 348 impact strength. The natural and synthetic reinforced composite (L-3) has impact strength of
 349 36.75 kJ/m^2 . Further as the filler concentration increases in hybridized composites resulted in
 350 decreased impact strength of 31.5 kJ/m^2 (L-4), 28.35 kJ/m^2 (L-5) and 24.93 kJ/m^2 (L-6). This
 351 was mainly due to the presence of filler material which reduces the compatibility of fiber-
 352 matrix interface and the adhesive nature between reinforcement and matrix phase.

353
$$\text{Impact strength (I.S)} = \frac{\text{Impact energy in Joules}}{\text{Area of crosssection in m}^2} \dots\dots\dots(\text{vii})$$

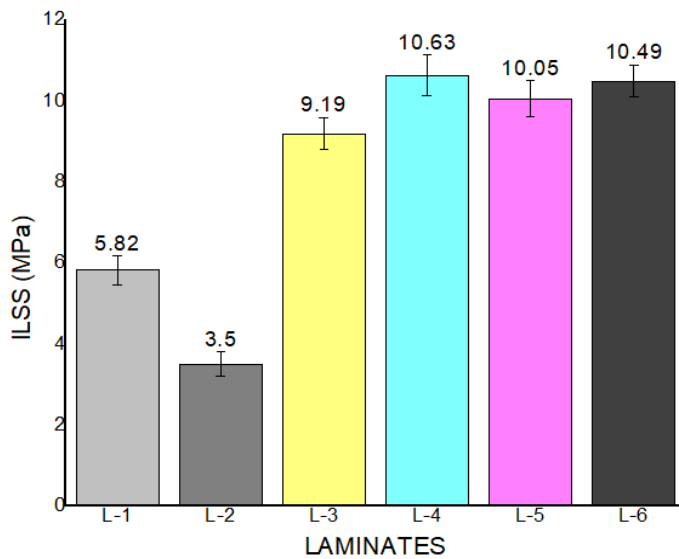


354
355 **Figure 5.** Impact strength of composites

356
357 **ILSS STUDIES**

358 The ILSS studies follows the flexural test method with shorter span length. The stress v/s
359 strain plots for ILSS specimens are shown in **S10**. The purpose of this test was to analyze the
360 bonding between the fibers and matrix and also to identify the breaking load of the specimen.
361 The load-displacement plot for different composite laminates are presented in **S11**. The
362 laminate L-2 withstands a lowest breaking load of 139 N in which failure of specimens
363 occurs by means breaking and bending of laminated fibers at lesser load capacity, whereas
364 the laminate L-1 containing sisal reinforcement achieves higher breaking load of 232 N
365 which was higher than the L-2 and thus indicating the strong bond between the fibers. The
366 hybridized laminate L-3 attains a load of 367 N which was higher than both the laminates L-1
367 and L-2. The load withstanding capacity was more in 2 % pp filled composite i.e., 425 N and
368 was higher among all the laminates prepared and further filler increased laminates L-5 and L-
369 6 resulted in breaking load of 399 N and 419 N respectively. The ILSS for the different
370 laminates are presented in **Figure 6**. The highest shear strength was achieved in L-4 (10.63

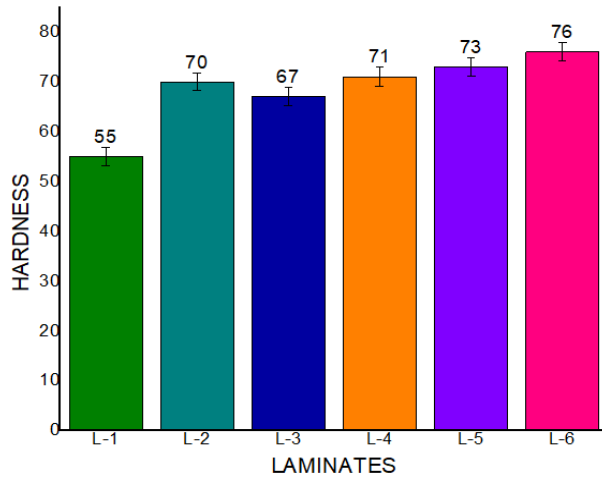
371 MPa) because of the existence of the filler particles which opposed the shearing of laminates
372 and hence enhanced strength of the laminates. The laminate L-2 showed a strength value of
373 3.5 MPa, while the other laminates L-1, L-5, L-6 had ILSS strength of 5.82 MPa, 10.05 MPa
374 and 10.49 MPa respectively. Hence it is concluded that the addition of fillers to hybridized
375 composite enhances the ILSS property.



376
377 **Figure 6.** ILSS of different composite laminates

378
379 **HARDNESS STUDIES**

380 **Figure 7** indicates the comparison of hardness values for different laminates using Shore-D
381 durometer. The laminate L-6 which consists of hybrid layers of sisal and kevlar with 6 %
382 filler material gives highest hardness value of 76 and 4 %, 2 % filler filled composite exhibits
383 hardness values ranging 73 and 71 respectively. This shows the filler material resistance
384 against the material deformation and the indentation of laminates. The other laminates L-1,
385 L-2 and L-3 hardness values ranged 55, 70 and 67 respectively. The natural sisal reinforced
386 composite showed least hardness value due to its softness which resulted in easier material
387 deformation.



388

389 **Figure 7.** Hardness value for different laminates

390

391 **WATER ABSORPTION STUDIES**

392 The specimens gain weight due to absorbing of water molecules after immersion. The test
 393 was conducted for a duration of 28 days in normal and distilled water with intervals of 7
 394 days. The weights before and after duration in both the conditions are tabulated in **Table 4**
 395 and **5**. The test results reveal that the water absorption percentage is more in L-
 396 1 laminate which is composed of pure sisal fabric. The less amount of water absorption is seen
 397 in laminate L-2 which contains 4 layers of kevlar fabrics. The plane hybridized composites
 398 exhibit less absorption capacity as opposed to filler filled laminate because of the natural
 399 fillers cellulose based content. The specimen's water absorption was more in normal water as
 400 compared to distilled water.

401 **Table 4.** Water absorption percentage in distilled water

Laminates	Weight of the specimens Before immersion (g)	Percentage increase in weights			
		Day 7	Day 14	Day 21	Day 28
L-1	4.286	7.12	9.25	13.78	16.69

L-2	3.776	2.36	5.02	8.26	11.53
L-3	3.987	3.27	6.38	10.24	13.92
L-4	4.126	3.38	6.95	10.97	14.02
L-5	4.187	3.76	7.23	11.26	14.43
L-6	4.215	4.01	7.91	11.95	14.93

402

403 **Table 5.** Water absorption percentage in normal water

Laminates	Weight of the specimens Before immersion (g)	Percentage increase in weights			
		Day 7	Day 14	Day 21	Day 28
L-1	4.395	6.9	9.65	13.98	17.08
L-2	3.721	2.64	5.56	8.95	12.01
L-3	3.921	3.26	7.02	10.98	14.03
L-4	4.105	3.86	7.27	11.23	14.82
L-5	4.196	4.03	8.12	12.12	14.96
L-6	4.296	4.4	8.3	12.35	15.56

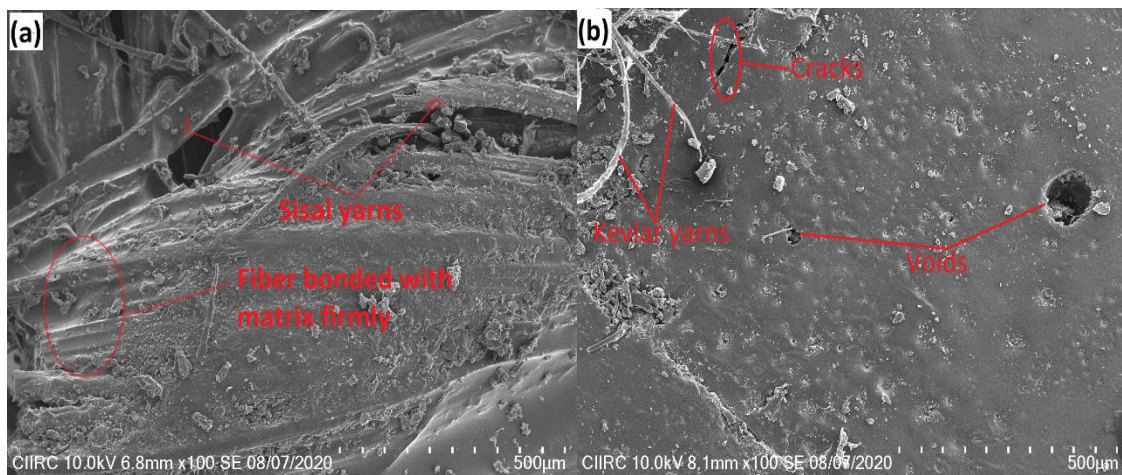
404

405

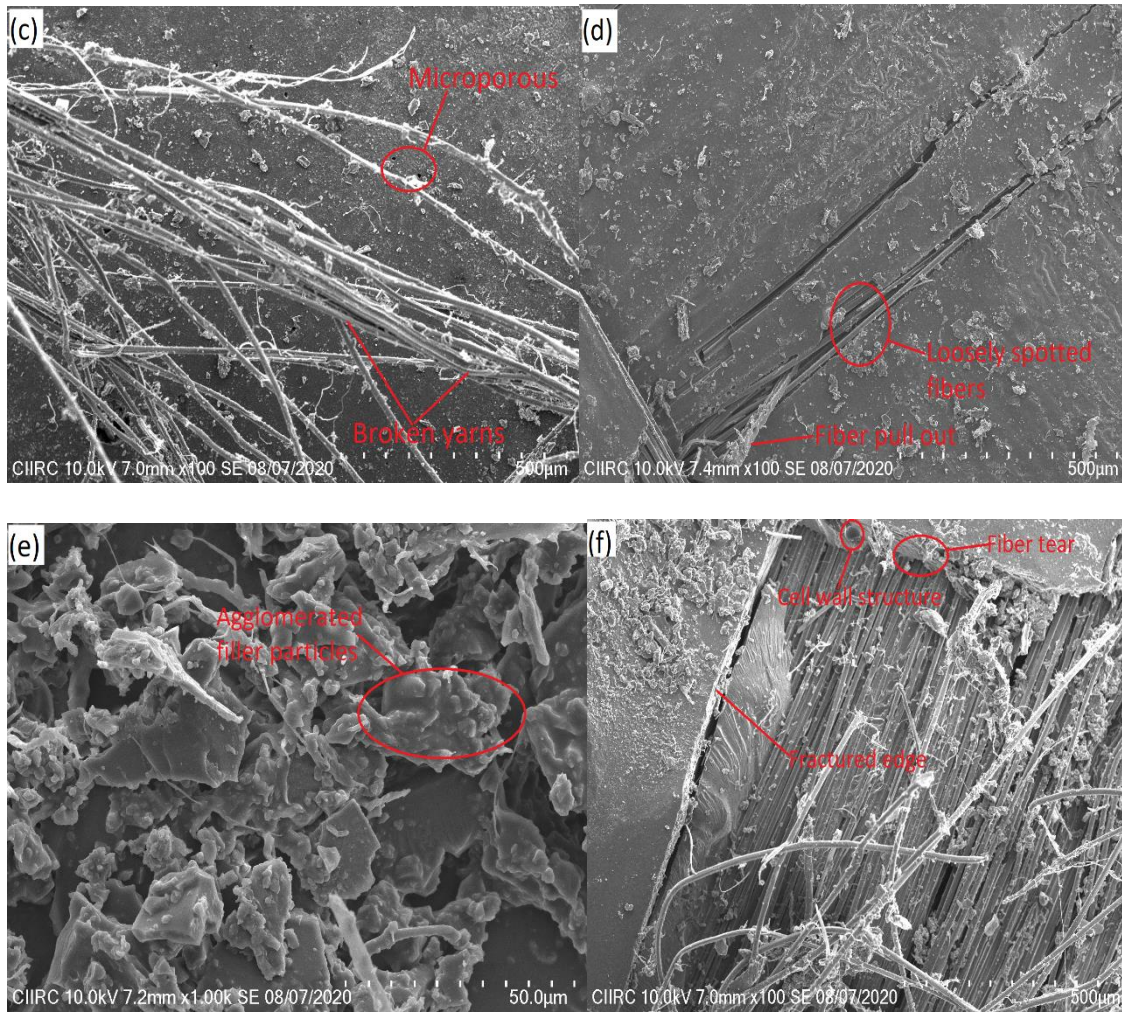
406 **SEM STUDIES**

407 The SEM studies was carried out for the analysis of composite fractured surfaces for the
408 examination of fiber-matrix bonding interface. The scanned SEM image was coated with
409 gold layer before image capturing. The tensile fractured SEM images of sisal/kevlar and filler
410 filled hybrid epoxy composites are shown in **Figure 10**. The sisal fiber yarns (L-1) bonded
411 with matrix material is shown in **Figure 10 (a)**. It is observed that smoother surfaces can be
412 found in the structure and some resin poor spaces were found around the yarns. **Figure 10 (b)**

413 indicates the micro image of kevlar fiber reinforced composite laminate (L-2) and broken
414 kevlar yarns are spotted in the figure. The voids were found on the surface of the specimen
415 and surface cracks were found due to less adhesive nature between fiber and the matrix.
416 **Figure 10 (c)** indicates the fractured surface of hybridized laminate (L-3) where fiber yarns
417 breakage occurred and indicated the better adhesion between the fibers and matrix. Some
418 small micro pores were observed in the image due to air bubbles which occurs commonly in
419 hand lay-up process. **Figure 10 (d)** indicates the existence of strong bonding between fiber-
420 matrix and the filler material. Lesser voids, fiber breakage was observed along with the fiber
421 pullout. The loosely spotted fiber area was observed due to weak strength between fiber and
422 the matrix. The filler particles agglomeration with the matrix was observed in **Figure 10 (e)**.
423 Sometimes the space was found around the yarns because of fiber diameter and alignment of
424 fabric manually. The cell wall structures were found where the fibers yarns are completely
425 pulled out from the matrix (**Figure 10 (f)**). Fiber tearing occurs during the tensile loading in
426 the poor strengthened area.



427



428

429

430 **Figure 10.** SEM micrographs of tensile fractured surfaces:(a) Laminate L-1; (b) Laminate L-

431 2; (c) Laminate L-3; (d) Laminate L-4; (e) Laminate L-5; (f) Laminate (L-6)

432

433 The fractured flexural specimens are presented in **Figure 11**. It was observed that during

434 flexural loading the fibers bending occurs whereas in some cases the fiber yarns pulled out

435 from the matrix phase and leaves the space which are mentioned as fiber yarn walls and are

436 indicated in **Figure 11 (a)**. The fractured edges are represented in **Figure 11 (b)**. Due to the

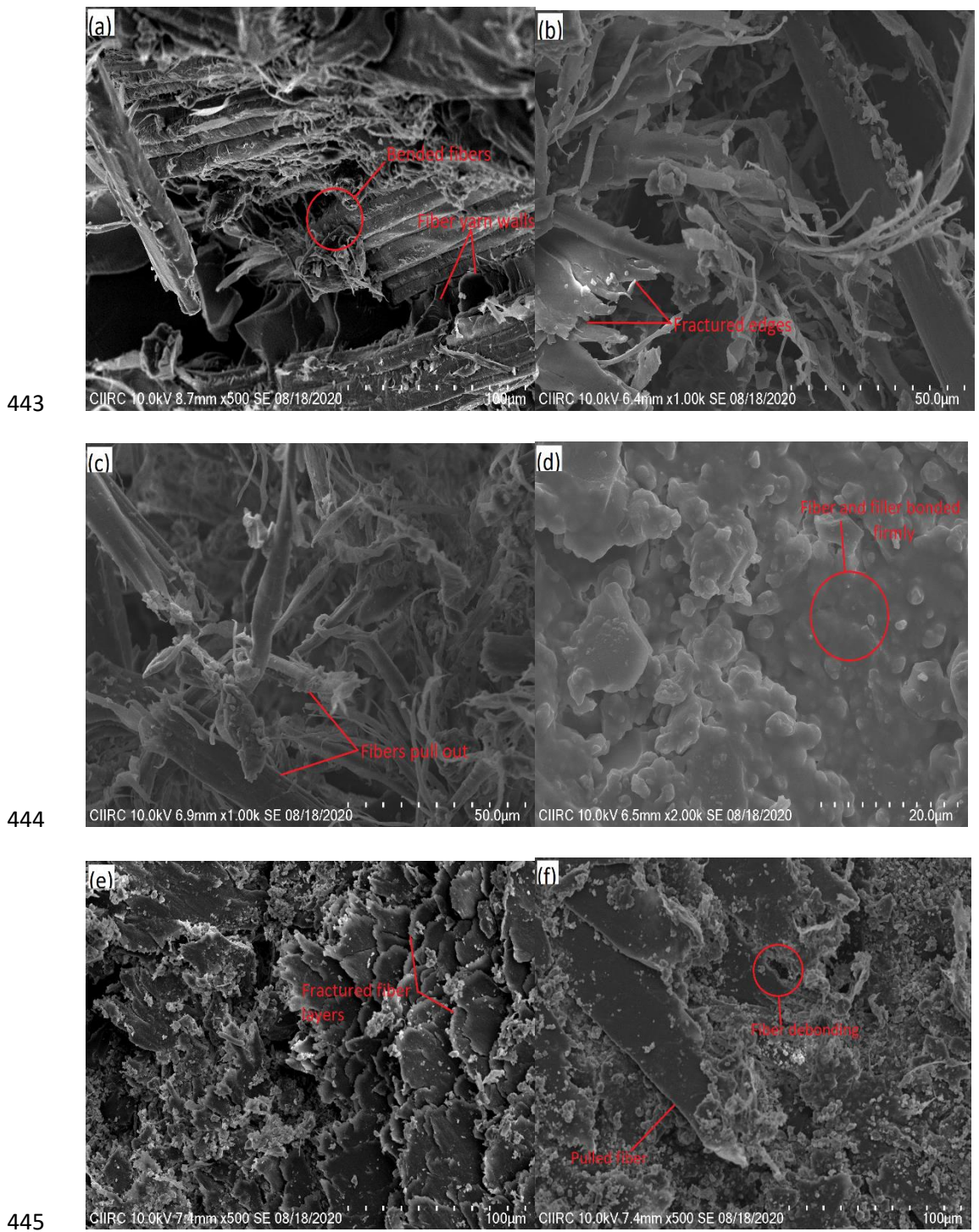
437 lesser interfacial adhesion, the fiber pullout occurred, and resin rich area was spotted in

438 **Figure 11 (c) and (d)** respectively. The weaker sections of the composite results in pull out of

439 the fibers from the matrix phase (**Figure 11 (e) and (f)**). As compared to tensile specimens

440 the voids and loosely bonded fibers are less in flexural specimens. Especially the filler filled

441 composite laminates exhibits less fiber breakage, crack propagation and higher adhesive
442 strength between fiber-matrix and the filler materials.



446 **Figure 11.** SEM morphology of flexural specimens: (a) Laminate L-1; (b) Laminate L-2; (c)
447 Laminate L-3; (d) Laminate L-4; (e) Laminate L-5; (f) Laminate (L-6)

448

449 **CONCLUSIONS**

450 In this experimental work, sisal/ kevlar fabrics were successfully reinforced with epoxy
451 matrix and were filled with 2%, 4% and 6% of pongamia pinnata to come up with a novel
452 material in the field of natural fiber polymer composites. Manual hand lay-up method was
453 employed in fabrication of the hybrid composite laminates and those prepared laminates were
454 scrutinized for their different physical, mechanical and microstructural properties. The
455 volume fraction studies deliberate that the L-6 laminates show lesser voids among all the
456 laminates due to the incorporation of kevlar fabric and filler material in natural sisal fabrics.
457 The superior tensile, flexural, impact and hardness properties of the prepared sisal/kevlar
458 filled pongamia pinnata reinforced hybrid composite laminates justifies their utilization in
459 some medium load structural applications. The water absorption study also exemplifies that
460 the addition of natural filler will significantly affect in the moisture resistance behaviour of
461 the prepared composites. The SEM morphology analysis reveals the strong bonding in filler-
462 based composites with lesser void contents which in turn envied the better adhesion
463 properties between fabrics and epoxy matrix impacting in better physico-mechanical
464 properties. Hence from all the test observations, the hybrid composite with 2 % filler gives
465 optimum results and hence recommended in some applications such as bicycle frames,
466 helmets, car door panels, computer spare parts, mobile cases, mats and office cubicle frames.

467

468 **ACKNOWLEDGEMENTS**

469 The authors would like to extend their sincere appreciation to the Researchers Supporting
470 Project for funding this work through Research Number (RSP-2020/138), King Saud
471 University, Riyadh, Saudi Arabia.

472

473

474 **Declarations**

475 **Funding:** The authors would like to extend their sincere appreciation to the Researchers
476 Supporting Project for funding this work through Research Number (RSP-2020/138), King
477 Saud University, Riyadh, Saudi Arabia.

478 **Conflicts of interest/Competing interests:** None

479 **Availability of data and material:** Not applicable

480 **Code availability:** Not applicable

481

482 **REFERENCES**

483 Amir SMM, Sultan MTH, Jawaid M, et al (2019) Nondestructive testing method for Kevlar
484 and natural fiber and their hybrid composites. In: *Durability and Life Prediction in*
485 *Biocomposites, Fibre-Reinforced Composites and Hybrid Composites*. Elsevier, pp 367–
486 388

487 Arpitha GR, Sanjay MR, Senthamaraikannan P, et al (2017) Hybridization effect of
488 sisal/glass/epoxy/filler based woven fabric reinforced composites. *Exp Tech* 41:577–584

489 Asim M, Jawaid M, Saba N, et al (2017) Processing of hybrid polymer composites—a
490 review. In: *Hybrid Polymer Composite Materials*. Elsevier, pp 1–22

491 Damião Xavier F, Santos Bezerra G, Florentino Melo Santos S, et al (2018) Evaluation of the
492 simultaneous production of xylitol and ethanol from sisal fiber. *Biomolecules* 8:2

493 Dinesh S, Kumaran P, Mohanamurugan S, et al (2020) Influence of wood dust fillers on the
494 mechanical, thermal, water absorption and biodegradation characteristics of jute fiber
495 epoxy composites. *J Polym Res* 27:9

496 Elanchezhian C, Ramnath BV, Ramakrishnan G, et al (2018) Review on mechanical
497 properties of natural fiber composites. *Mater Today Proc* 5:1785–1790

498 Fu S, Yu B, Tang W, et al (2018) Mechanical properties of polypropylene composites
499 reinforced by hydrolyzed and microfibrillated Kevlar fibers. *Compos Sci Technol*
500 163:141–150

501 Gowda TGY, Sanjay MR, Bhat KS, et al (2018) Polymer matrix-natural fiber composites: An
502 overview. *Cogent Eng* 5:1446667

503 HPS AK, Masri M, Saurabh CK, et al (2017) Incorporation of coconut shell based
504 nanoparticles in kenaf/coconut fibres reinforced vinyl ester composites. *Mater Res*
505 *Express* 4:35020

506 Jani SP, Kumar AS, Khan MA, Kumar MU (2016) Machinability of hybrid natural fiber
507 composite with and without filler as reinforcement. *Mater Manuf Process* 31:1393–1399

508 Jothibas S, Mohanamurugan S, Vijay R, et al (2020) Investigation on the mechanical
509 behavior of areca sheath fibers/jute fibers/glass fabrics reinforced hybrid composite for
510 light weight applications. *J Ind Text* 49:1036–1060.
511 <https://doi.org/10.1177/1528083718804207>

512 Madhu P, Sanjay MR, SenthamaraiKannan P, et al (2019) A review on synthesis and
513 characterization of commercially available natural fibers: Part II. *J Nat Fibers* 16:25–36

514 Matykiewicz D, Barczewski M, Knapski D, Skórczewska K (2017) Hybrid effects of basalt
515 fibers and basalt powder on thermomechanical properties of epoxy composites. *Compos*
516 *Part B Eng* 125:157–164

517 Mohan N, Natarajan S, KumareshBabu SP (2012) The role of synthetic and natural fillers on
518 three-body abrasive wear behaviour of glass fabric–epoxy hybrid composites. *J Appl*
519 *Polym Sci* 124:484–494

520 Naveen J, Jawaid M, Amuthakkannan P, Chandrasekar M (2019) Mechanical and physical
521 properties of sisal and hybrid sisal fiber-reinforced polymer composites. In: *Mechanical*
522 *and physical testing of biocomposites, fibre-reinforced composites and hybrid*

523 composites. Elsevier, pp 427–440

524 Ojha S, Raghavendra G, Acharya SK (2014) A comparative investigation of bio waste filler
525 (wood apple-coconut) reinforced polymer composites. *Polym Compos* 35:180–185

526 Prabu VA, Manikandan V, Uthayakumar M, Kalirasu S (2012) Investigations on the
527 mechanical properties of red mud filled sisal and banana fiber reinforced polyester
528 composites. *Mater Phys Mech* 15:173–179

529 Praveenkumara J, Madhu P, Yashas Gowda TG, Pradeep S Studies on Mechanical Properties
530 of Bamboo/Carbon Fiber Reinforced Epoxy Hybrid Composites Filled with SiC
531 Particulates

532 Qi HJ, Joyce K, Boyce MC (2003) Durometer hardness and the stress-strain behavior of
533 elastomeric materials. *Rubber Chem Technol* 76:419–435

534 Rajulu AV, Chary KN, Reddy GR, Meng YZ (2004) Void content, density and weight
535 reduction studies on short bamboo fiber–epoxy composites. *J Reinf Plast Compos*
536 23:127–130

537 Rana RS, Rana S, Purohit R (2017) Characterization of properties of epoxy sisal/glass fiber
538 reinforced hybrid composite. *Mater Today Proc* 4:5445–5451

539 Sanjay MR, Arpitha GR, Laxmana Naik L, et al (2016) Studies on mechanical properties of
540 banana/e-glass fabrics reinforced polyester hybrid composites. *J Mater Environ Sci*
541 7:3179–3192

542 Sanjay MR, Madhu P, Jawaid M, et al (2018) Characterization and properties of natural fiber
543 polymer composites: A comprehensive review. *J Clean Prod* 172:566–581

544 Sanjay MR, Siengchin S, Parameswaranpillai J, et al (2019) A comprehensive review of
545 techniques for natural fibers as reinforcement in composites: Preparation, processing and
546 characterization. *Carbohydr Polym* 207:108–121.
547 <https://doi.org/10.1016/j.carbpol.2018.11.083>

548 Shakuntala O, Raghavendra G, Samir Kumar A (2014) Effect of filler loading on mechanical
549 and tribological properties of wood apple shell reinforced epoxy composite. *Adv Mater*
550 *Sci Eng* 2014:

551 Sharma V, Meena ML, Kumar M (2020) Effect of filler percentage on physical and
552 mechanical characteristics of basalt fiber reinforced epoxy based composites. *Mater*
553 *Today Proc*

554 Singh H, Batra NK, Dikshit I (2020) Development of new hybrid jute/carbon/fishbone
555 reinforced polymer composite. *Mater Today Proc*

556 Swolfs Y, Gorbatiikh L, Verpoest I (2014) Fibre hybridisation in polymer composites: a
557 review. *Compos Part A Appl Sci Manuf* 67:181–200

558 Thyavihalli Girijappa YG, Mavinkere Rangappa S, Parameswaranpillai J, Siengchin S (2019)
559 Natural Fibers as Sustainable and Renewable Resource for Development of Eco-
560 Friendly Composites: A Comprehensive Review. *Front Mater* 6:1–14.
561 <https://doi.org/10.3389/fmats.2019.00226>

562 Vinod A, Sanjay MR, Siengchin S, Parameswaranpillai J (2020) Renewable and Sustainable
563 Biobased Materials: An Assessment on Biofibers , Biofilms , Biopolymers and
564 Biocomposites. *J Clean Prod* 258:120978. <https://doi.org/10.1016/j.jclepro.2020.120978>
565

Figures



(a)



(b)



(c)



(d)

Figure 1

Materials used in the present study: (a) sisal fabric (b) kevlar fabric (c) *Pongamia pinnata* shells (d) *Pongamia pinnata* shells powder

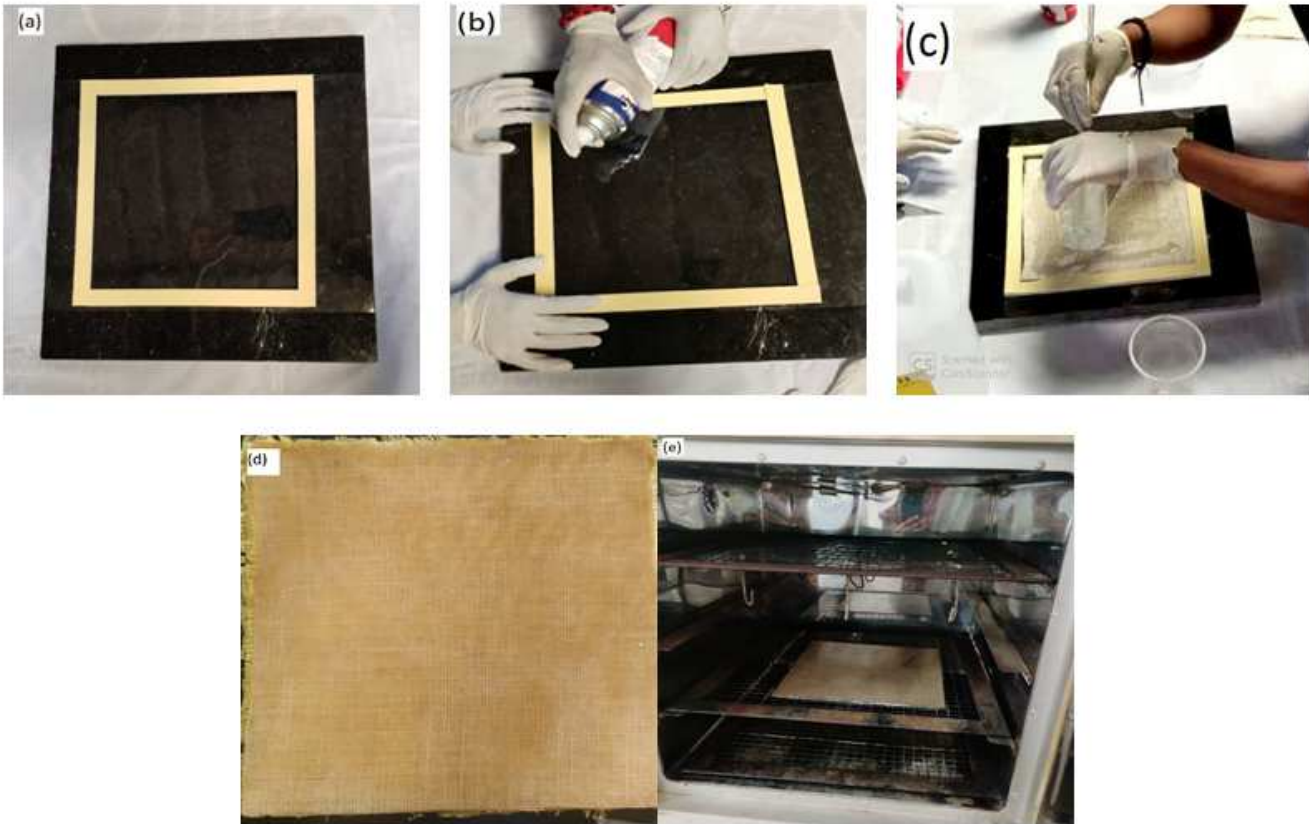
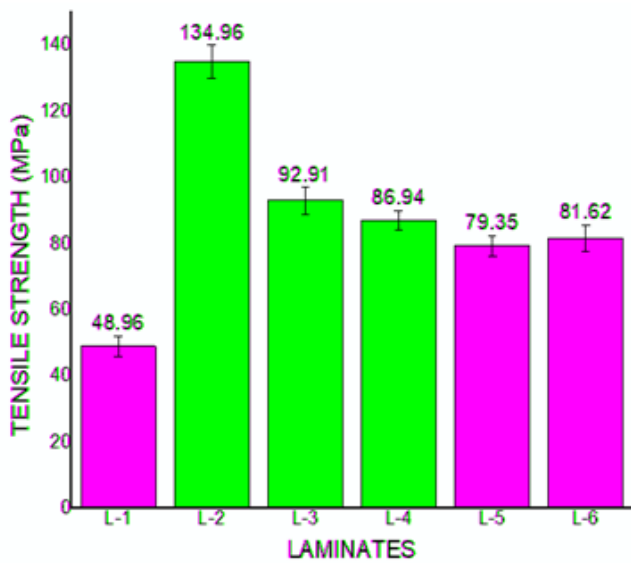
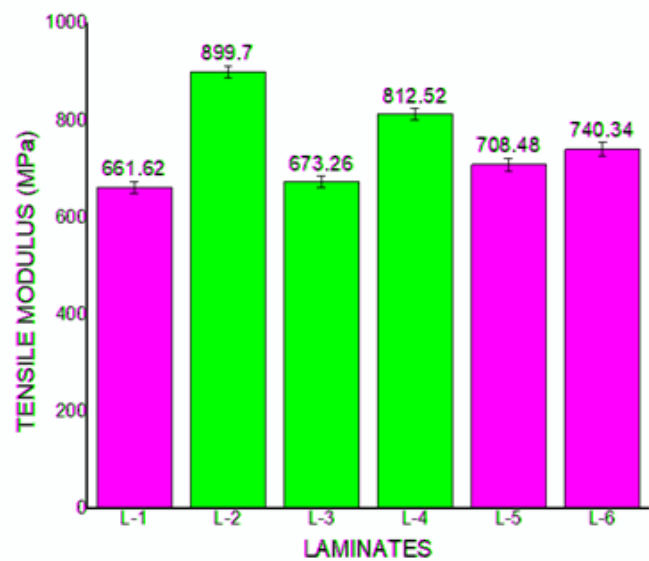


Figure 2

(a) Mold prepared using sealing tape (b) Silicone spray (c) Resin lay up (d) Fabricated laminate (e) Laminate curing in oven.



(a)



(b)

Figure 3

Tensile test results of the laminates: (a) Tensile strength (b) Tensile modulus

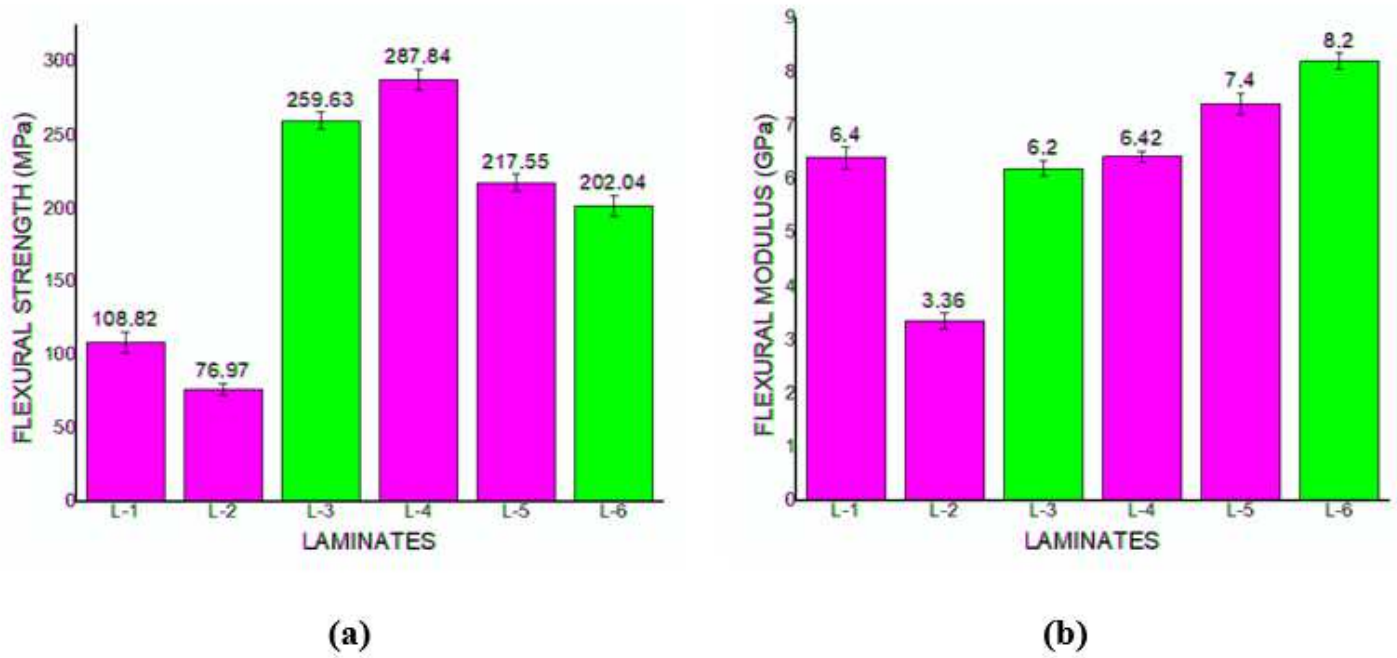


Figure 4

Flexural test results of the laminates: (a) Flexural strength (b) Flexural modulus

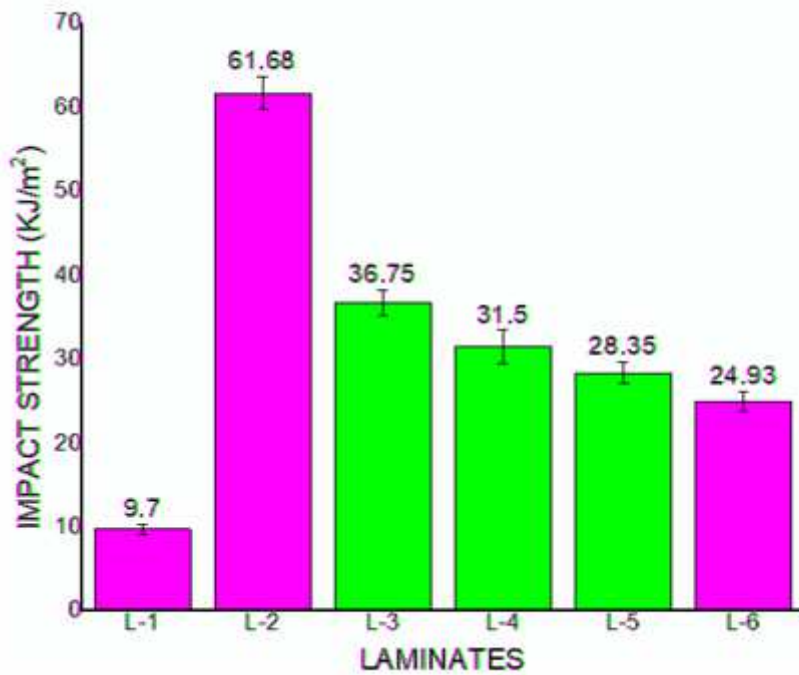


Figure 5

Impact strength of composites

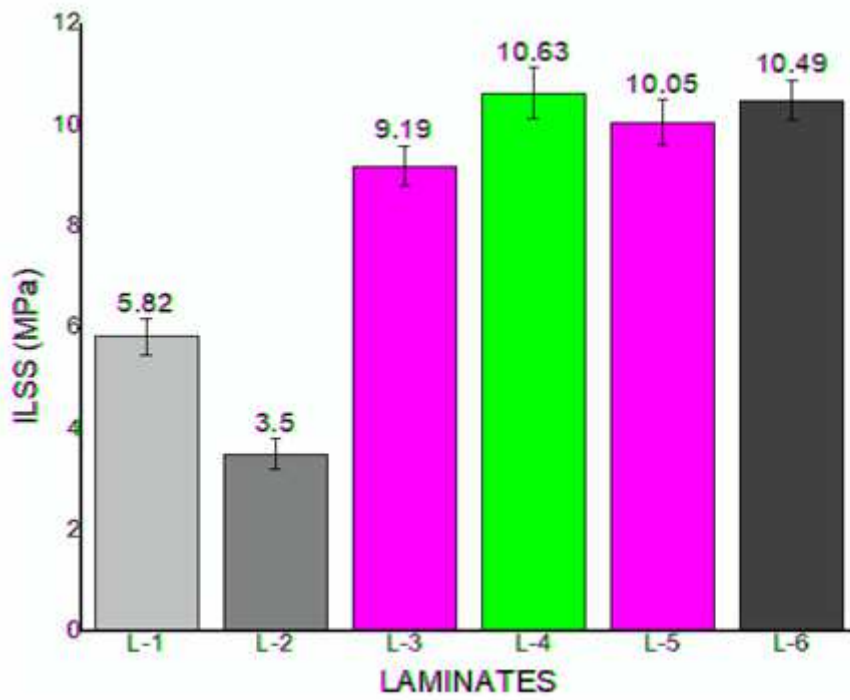


Figure 6

ILSS of different composite laminates

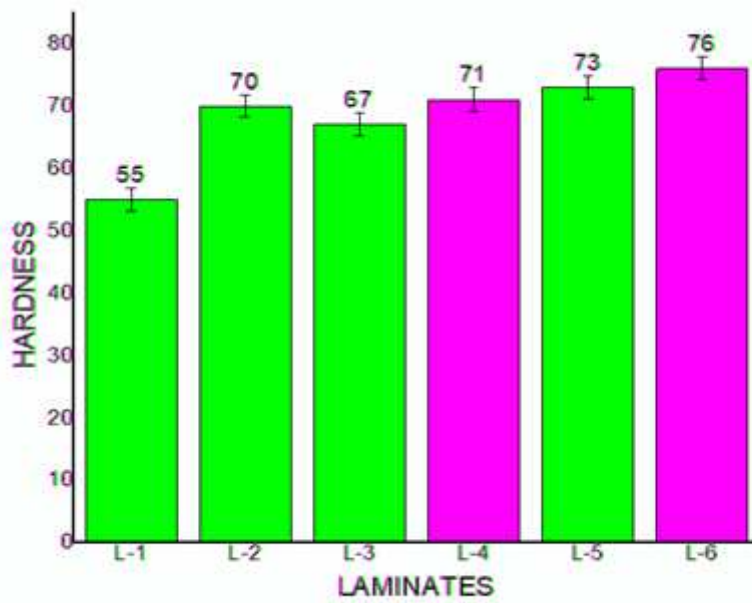


Figure 7

Hardness value for different laminates

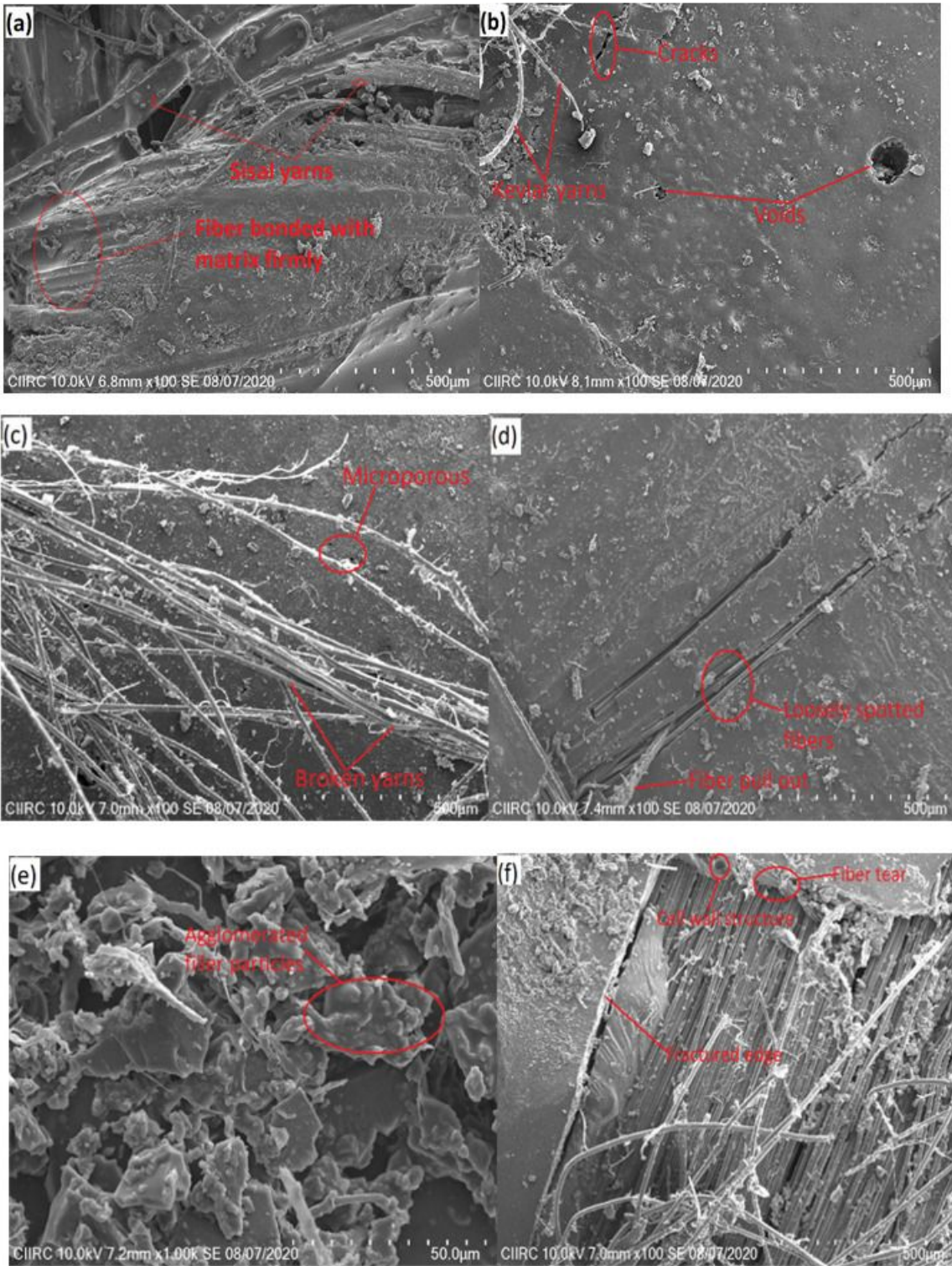


Figure 8

SEM micrographs of tensile fractured surfaces:(a) Laminate L-1; (b) Laminate L-2; (c) Laminate L-3; (d) Laminate L-4; (e) Laminate L-5; (f) Laminate (L-6)

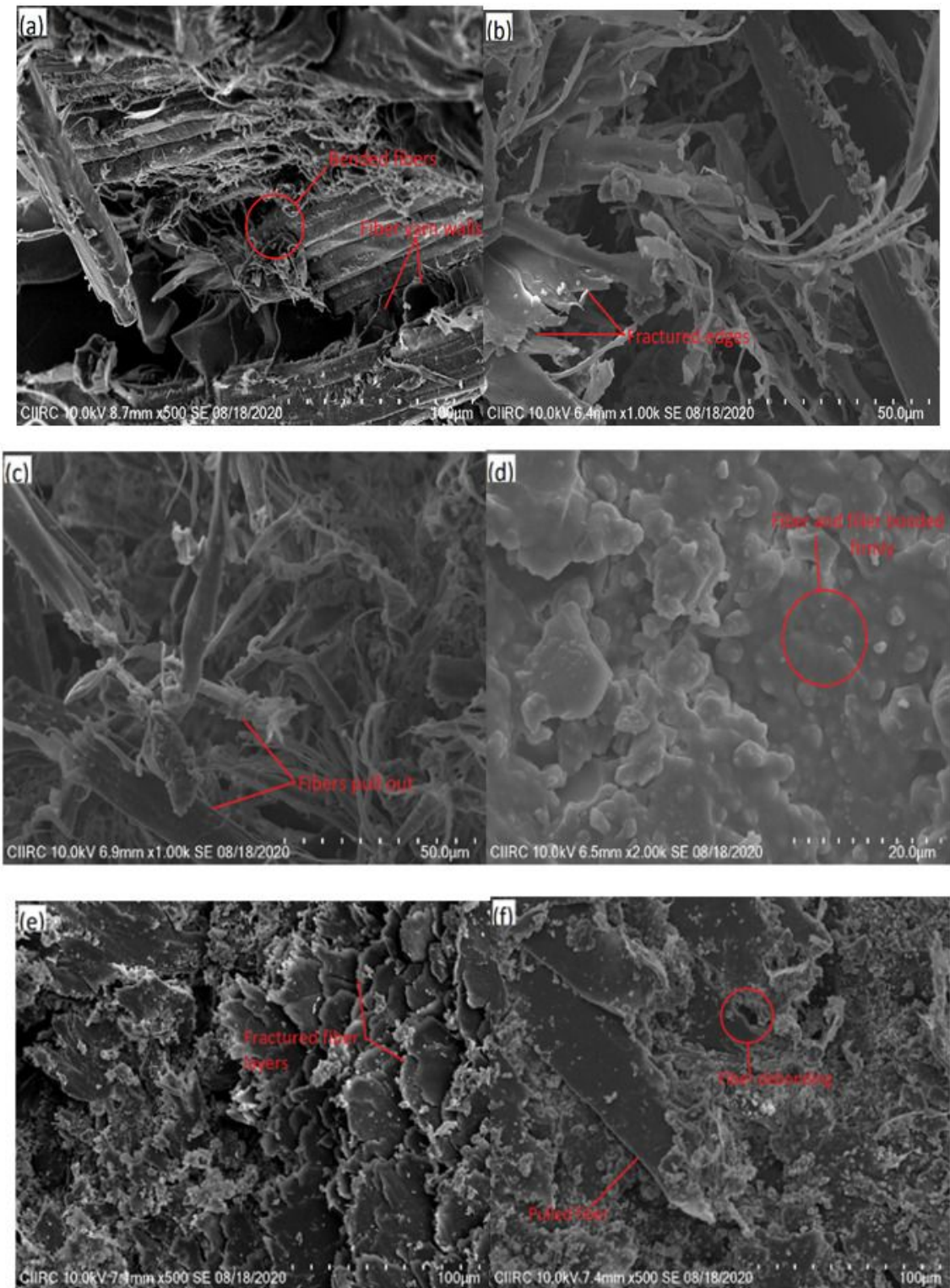


Figure 9

SEM morphology of flexural specimens: (a) Laminate L-1; (b) Laminate L-2; (c) Laminate L-3; (d) Laminate L-4; (e) Laminate L-5; (f) Laminate (L-6)

Supplementary Files

This is a list of supplementary files associated with this preprint. Click to download.

- [SupplymentaryMaterials.docx](#)